Available online at www.sciencedirect.com
ScienceDirect
Journal of Sound and Vibration 313 (2008) 875–890
JOURNAL OF SOUND AND VIBRATION
www.elsevier.com/locate/jsvi

# Free vibration and buckling of composite beams with interlayer slip by two-dimensional theory

Rongqiao Xu[a], Yu-Fei Wu[b,*]

[a]Department of Civil Engineering, Zhejiang University, Hangzhou 310027, China
[b]Department of Building and Construction, City University of Hong Kong, Tat Chee Avenue, Kowloon, Hong Kong, China

Received 31 August 2007; received in revised form 7 December 2007; accepted 15 December 2007
Handling Editor: L.G. Tham
Available online 19 February 2008

**Abstract**

The free vibration and buckling of partial interaction composite beams are investigated using the state-space method based on the two-dimensional theory of elasticity. The analytical solutions of a beam with two simply supported ends are obtained as well as semi-analytical solutions are obtained for other end conditions using the differential quadrature method coupled with the state-space method. The frequencies and buckling loads are tabulated and compared with those available in the literature. Because the plane section assumption of the classical beam theory is not used, the presented method is applicable not only to slender beams, but also to thick beams. Consequently, the presented method can be a benchmark for other approximate methods based on one-dimensional beam theories.


## 1. Introduction

Partial interaction composite members have attracted much research attention due to their more complex behavior, which is caused by the interlayer slip between the individual components. Newmark et al. [1] presented the linear relationship of the interlayer slip and the rigidity of the shear connector based on their experiment results. Following this famous work, many interesting and useful results have been obtained by using analytical, numerical, or experimental methods. For example, Goodman [2], Girhammar and Gopu [3] and Girhammar and Pan [4,5], Wang [6], Biscontin et al. [7], Ranzi and Bradford [8], Wu et al. [9,10], and Chen et al. [11] have presented analytical investigations concerning the static or dynamic behavior of composite beams with interlayer slip. Amana and Booth [12] and Wu et al. [13] have designed experiments and investigated the experimental results to demonstrate analytical methods. In addition, many researchers have presented the beam elements including the effects of partial interaction [14–17]. All of the above-mentioned methods are based on Euler–Bernoulli beam theory and are applicable only to slender beams or low order vibration in beams. Schnabl et al. [18] analyzed the static behavior of two-layer beams with partial interaction interface and shear deformation. Xu and Wu [19] investigated the static, dynamic, and buckling behavior of

*Corresponding author. Tel.: +852 2784 4259; fax: +852 2788 7612.
*E-mail address:* yfwu00@cityu.edu.hk (Y.-F. Wu).

0022-460X/$ - see front matter © 2007 Elsevier Ltd. All rights reserved.
doi:10.1016/j.jsv.2007.12.029

partial interaction composite beams using Timoshenko's beam theory (TBT). These works demonstrated the effects of shear deformation and rotational inertia on the deflections and vibration frequencies of partial interaction composite beams. Berczynski and Wrsblewski [20] and Ranzi and Zona [21] also analyzed the vibration of steel–concrete composite beams using Timoshenko beam model.

Xu and Wu [22] presented a plane stress model of composite beams with interlayer slip by the state-space method based on two-dimensional theory. The deflection and stress are obtained analytically for a beam with two simply supported ends under arbitrarily distributed transverse loading. Their method discards the plane section assumption of the classical beam theory (CBT) and can predict the static behavior of partial interaction composite beams more precisely than existing beam theories, especially for a thick beam. In this paper, the state-space method is extended to investigate the free vibration and buckling of partial interaction composite beams. The exact analytical solution of beams with two simply supported ends is obtained through trigonometric function expansion. Moreover, the solution of beams with non-simply supported ends is solved by a semi-analytical method using the differential quadrature method (DQM) coupled with state-space method, which was first presented by Chen and co-workers [23,24] and called SS-DQM. Finally, the numerical results are tabulated to compare the analytical and semi-analytical methods.

## 2. Formulation

The main idea of the previous work [22] is given in brief and then extended for the vibration and buckling analysis of composite beams. Fig. 1(a) shows a composite beam that consists of sub-elements with different material properties. By employing the equivalent rules presented in the previous work [22], the Young's moduli $E_i'$ of the realistic materials are converted to the equivalent moduli $E_i$ through multiplying the corresponding width $b_i$. To investigate the dynamic behavior of the beams, the densities $\rho_i'$ of the realistic materials must also be converted to the equivalent densities $\rho_i$, which can be readily obtained through multiplying the width $b_i$ again, for considering the inertial force. Finally, the dimensions and material properties of the equivalent cross section are shown in Fig. 1(b). In this way, the composite beam is converted to a plane stress state [22,25].

To study the buckling behavior of the composite member, the axial force needs to be taken into account in the above model. However, the axial force as a stress resultant cannot be applied directly to the plane stress problem, because only the stress and displacement components exist in the governing equation and boundary conditions. In other words, the axial force must be treated as an initial normal stress in the axial direction according to Saint Venant's principle. Fig. 2(a) shows one end of the composite beam with an axial force $N_{x0}$, which is located at the neutral axis of the beam. It is well known that the axial force $N_{x0}$ can be replaced by a static equivalent distributed stress $\sigma_{xi}^0$ (as shown in Fig. 2(b)) in which only the stresses near the end are affected, in accordance with Saint Venant's principle.

Based on the foregoing analysis, a two-dimensional model is proposed for partial interaction composite beams, as shown in Fig. 3. The model is assumed to have $m$ elements in general, because some members, such as the steel I-type section, need to be treated as multiple elements due to the different widths of its flange and

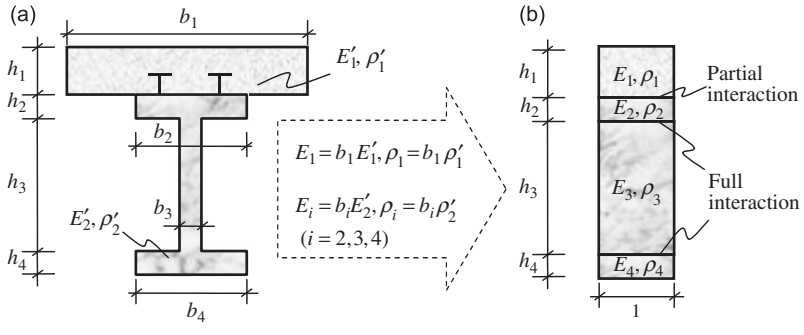


Fig. 1. Original and equivalent cross sections of composite beams.

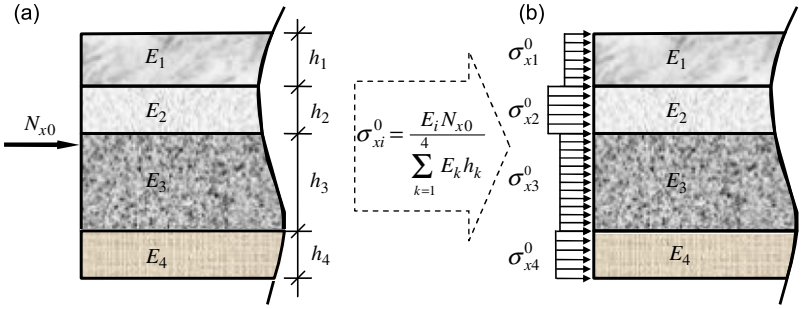


Fig. 2. The axial force and equivalent axial stress according to Saint Venant's principle.

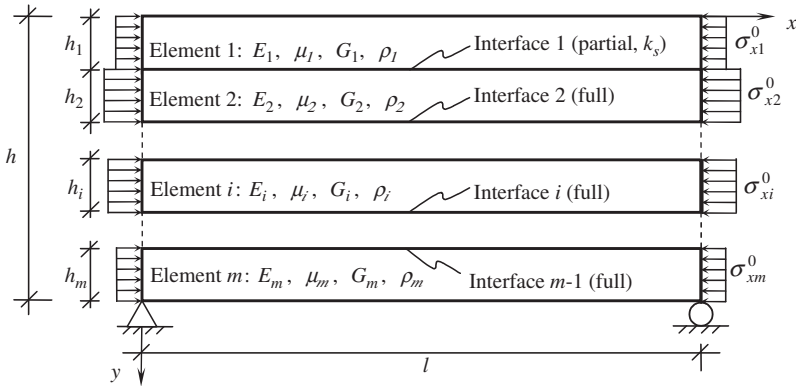


Fig. 3. Two-dimensional model of partial interaction composite beams.

web (see Fig. 1). The symbols $E_i$, $\mu_i$, $G_i$, $\rho_i$, and $h_i$ denote the elastic modulus, Poisson's ratio, shear modulus, mass density, and height of element $i$, respectively. In the following derivation, it is further assumed that the interlayer slip occurs at interface 1 of elements 1 and 2, and that the other interfaces are perfectly bonded. For interlayer slips that exist at other interfaces, the presented method is similarly applicable. The rigidity of the shear connector is denoted by $k_s$, and $\sigma_{xi}^0$ is the initial stress applied on the $i$th element converted from the axial force.

The differential equation of motion with the initial stress for the plane stress state in the $xy$ plane of element $i$ is given by

$$\begin{aligned}\frac{\partial \sigma_{xi}}{\partial x}+\frac{\partial \tau_{xyi}}{\partial y}&=\rho_i\frac{\partial^2 u_i}{\partial t^2}+\sigma_{xi}^0\frac{\partial^2 u_i}{\partial x^2},\\ \frac{\partial \tau_{xyi}}{\partial x}+\frac{\partial \sigma_{yi}}{\partial y}&=\rho_i\frac{\partial^2 v_i}{\partial t^2}+\sigma_{xi}^0\frac{\partial^2 v_i}{\partial x^2},\end{aligned}\tag{1}$$

where $\sigma_{xi}$ and $\sigma_{yi}$ are the normal stresses and $\tau_{xyi}$ is the shear stress of element $i$. The constitutive relations of an isotropic material are given by

$$\frac{\partial u_i}{\partial x}=\frac{1}{E_i}\left[\sigma_{xi}-\mu_i\sigma_{yi}\right],\quad \frac{\partial v_i}{\partial y}=\frac{1}{E_i}\left[-\mu_i\sigma_{xi}+\sigma_{yi}\right],\quad \frac{\partial u_i}{\partial y}+\frac{\partial v_i}{\partial x}=\frac{1}{G_i}\tau_{xyi}\tag{2}$$

in which $u_i$ and $v_i$ are the longitudinal and transverse displacements of element $i$, respectively. The governing equations (1) and (2) of the plane stress problem include three stresses $\sigma_{xi}$, $\sigma_{yi}$, and $\tau_{xyi}$ and two displacements $u_i$ and $v_i$. They can be rearranged into the so-called state-space formula through substitutions and

simplifications in a way similar to that detailed in the previous work [22,25], i.e.,

$$\frac{\partial}{\partial y}\begin{Bmatrix} u_i \\ \sigma_{yi} \\ v_i \\ \tau_{xyi} \end{Bmatrix} = \begin{bmatrix} 0 & 0 & -\partial/\partial x & 1/G_i \\ 0 & 0 & \beta_i & -\partial/\partial x \\ -\mu_i\partial/\partial x & (1-\mu_i^2)/E_i & 0 & 0 \\ \beta_i - E_i\partial^2/\partial x^2 & -\mu_i\partial/\partial x & 0 & 0 \end{bmatrix} \begin{Bmatrix} u_i \\ \sigma_{yi} \\ v_i \\ \tau_{xyi} \end{Bmatrix} \tag{3}$$

which is called the state-space formula of the plane stress problem of element $i$, in which the quantities $u_i$, $\sigma_{yi}$, $v_i$, and $\tau_{xyi}$ are the state variables. The equation $\beta_i = \rho_i\partial^2/\partial t^2 + \sigma_{xi}^0\partial^2/\partial x^2$ is used to simplify the expressions. Let $\beta_i$ equal zero and Eq. (3) can be reduced to a static problem, which has been obtained in Ref. [22]. Another stress $\sigma_{xi}$ is called the derived variable and can be expressed in terms of the state variables $u_i$ and $\sigma_{yi}$ from the first one of Eq. (2) as

$$\sigma_{xi} = E_i\frac{\partial u_i}{\partial x} + \mu_i\sigma_{yi}. \tag{4}$$

Thus, the initial governing equations (1) and (2) become the state-space formula (3) and auxiliary equation (4), which is more convenient for solving the problem of laminated or composite beams.

## 3. Solution of beams with two simply supported ends

If a beam is simply supported at the two ends, the boundary conditions are

$$v_i = 0, \quad \sigma_{xi} = 0 \text{ at } x = 0 \text{ and } l. \tag{5}$$

The above boundary conditions are applicable to each element in the $y$ direction. This set of conditions is therefore more rigorous than that of one-dimensional beam theory in which a beam is only supported in a point-wise manner. Thus, the state variables can be assumed as

$$\begin{aligned} u_i &= hU_i(\zeta)\cos(n\pi\xi)\exp(\mathrm{j}\omega t), \quad \sigma_{yi} = E_0\sigma_i(\zeta)\sin(n\pi\xi)\exp(\mathrm{j}\omega t), \\ v_i &= hV_i(\zeta)\sin(n\pi\xi)\exp(\mathrm{j}\omega t), \quad \tau_{xyi} = E_0\tau_i(\zeta)\cos(n\pi\xi)\exp(\mathrm{j}\omega t), \end{aligned} \tag{6}$$

where $n$ denotes the half-wavenumber in the $x$ direction, $E_0$ is the parameter with the dimension of stress and is used to obtain the non-dimensional formulae, $\omega$ signifies the resonant frequency, and $t$ denotes time. The symbols $\xi$ and $\zeta$ denote the non-dimensional coordinates corresponding to $x$ and $y$, which are defined as

$$\xi = x/l, \quad \zeta = y/h. \tag{7}$$

Substituting Eq. (6) into Eq. (3) gives

$$\frac{\mathrm{d}}{\mathrm{d}\zeta}\begin{Bmatrix} U_i \\ \sigma_i \\ V_i \\ \tau_i \end{Bmatrix} = \begin{bmatrix} 0 & 0 & -\alpha_n & 1/\overline{G}_i \\ 0 & 0 & -\overline{\rho}_i\Omega^2 - \overline{\sigma}_{xi}^0\alpha_n^2 & \alpha_n \\ \mu_i\alpha_n & (1-\mu_i^2)/\overline{E}_i & 0 & 0 \\ -\overline{\rho}_i\Omega^2 + (\overline{E}_i - \overline{\sigma}_{xi}^0)\alpha_n^2 & -\mu_i\alpha_n & 0 & 0 \end{bmatrix} \begin{Bmatrix} U_i \\ \sigma_i \\ V_i \\ \tau_i \end{Bmatrix}, \tag{8}$$

where

$$\begin{aligned} &\alpha_n = n\pi h/l, \quad \overline{G}_i = G_i/E_0, \quad \overline{E}_i = E_i/E_0, \quad \overline{\sigma}_{xi}^0 = \sigma_{xi}^0/E_0, \quad \overline{\rho}_i = \rho_i/\rho_0, \\ &\Omega^2 = \rho_0\omega^2h^2/E_0 \end{aligned} \tag{9}$$

in which $\Omega$ is the non-dimensional frequency and $\rho_0$ is a parameter with the dimension of mass density. The stress $\sigma_{xi}$ is obtained by substituting Eq. (6) into Eq. (4) to give

$$\sigma_{xi} = E_0\left[-\alpha_n\overline{E}_iU_i(\zeta) + \mu_i\sigma_i(\zeta)\right]\sin(n\pi\xi)\exp(\mathrm{j}\omega t). \tag{10}$$

Consequently, it is readily found that the boundary conditions at the two ends are satisfied. Now Eq. (8) is an ordinary differential equation set and its solution is given by

$$\begin{Bmatrix} U_i(\zeta) \\ \sigma_i(\zeta) \\ V_i(\zeta) \\ \tau_i(\zeta) \end{Bmatrix} = \mathrm{e}^{[\boldsymbol{K}_i](\zeta-\zeta_{i-1})} \begin{Bmatrix} U_i(\zeta_{i-1}) \\ \sigma_i(\zeta_{i-1}) \\ V_i(\zeta_{i-1}) \\ \tau_i(\zeta_{i-1}) \end{Bmatrix} \quad (\zeta \in [\zeta_{i-1}, \zeta_i]) \tag{11}$$

in which $\zeta_0 = 0$, $\zeta_i = (h_1 + h_2 + \cdots + h_i)/h$ $(i = 1,2,\ldots,m)$, and the matrix $[\mathbf{K}_i]$ is the coefficient matrix of Eq. (8), namely,

$$[\mathbf{K}_i] = \begin{bmatrix} 0 & 0 & -\alpha_n & 1/\overline{G}_i \\ 0 & 0 & -\overline{\rho}_i\Omega^2 - \overline{\sigma}^0_{xi}\alpha_n^2 & \alpha_n \\ \mu_i\alpha_n & (1-\mu_i^2)/\overline{E}_i & 0 & 0 \\ -\overline{\rho}_i\Omega^2 + (\overline{E}_i - \overline{\sigma}^0_{xi})\alpha_n^2 & -\mu_i\alpha_n & 0 & 0 \end{bmatrix}. \tag{12}$$

Eq. (11) establishes a relation of the state variables at the location of $\zeta_{i-1}$ to $\zeta$ of element $i$. The exponential function of the matrix $[\mathbf{K}_i](\zeta-\zeta_i)$ is also a matrix, which is known as the transfer matrix through which the state variables are transferred from $\zeta_{i-1}$ to $\zeta$.

For the composite beam shown in Fig. 3, the compatibility conditions with interlayer slip at interface 1 are [22]

$$v_2(\zeta_1) = v_1(\zeta_1), \quad \sigma_{y2}(\zeta_1) = \sigma_{y1}(\zeta_1), \quad k_s[u_2(\zeta_1) - u_1(\zeta_1)] = \tau_{xy2}(\zeta_1) = \tau_{xy1}(\zeta_1) \tag{13}$$

and the continuous conditions of the other perfectly bonded interfaces are

$$\begin{aligned} &u_{i+1}(\zeta_i) = u_i(\zeta_i), \quad v_{i+1}(\zeta_i) = v_i(\zeta_i), \\ &\sigma_{y,i+1}(\zeta_i) = \sigma_{yi}(\zeta_i), \quad \tau_{xy,i+1}(\zeta_i) = \tau_{xyi}(\zeta_i) \end{aligned} \quad (i = 2,3,\ldots,m-1). \tag{14}$$

They can also be expanded in terms of the trigonometric function as in Eq. (6). Thus, the equivalent expressions of Eqs. (13) and (14) can be rewritten as

$$\begin{Bmatrix} U_2(\zeta_1) \\ \sigma_2(\zeta_1) \\ V_2(\zeta_1) \\ \tau_2(\zeta_1) \end{Bmatrix} = \begin{bmatrix} 1 & 0 & 0 & E_0/(k_s h) \\ 0 & 1 & 0 & 0 \\ 0 & 0 & 1 & 0 \\ 0 & 0 & 0 & 1 \end{bmatrix} \begin{Bmatrix} U_1(\zeta_1) \\ \sigma_1(\zeta_1) \\ V_1(\zeta_1) \\ \tau_1(\zeta_1) \end{Bmatrix} = [\mathbf{P}] \begin{Bmatrix} U_1(\zeta_1) \\ \sigma_1(\zeta_1) \\ V_1(\zeta_1) \\ \tau_1(\zeta_1) \end{Bmatrix} \tag{15}$$

and

$$\begin{Bmatrix} U_{i+1}(\zeta_i) \\ \sigma_{i+1}(\zeta_i) \\ V_{i+1}(\zeta_i) \\ \tau_{i+1}(\zeta_i) \end{Bmatrix} = \begin{Bmatrix} U_i(\zeta_i) \\ \sigma_i(\zeta_i) \\ V_i(\zeta_i) \\ \tau_i(\zeta_i) \end{Bmatrix} \quad (i = 2,3,\ldots,m-1). \tag{16}$$

If the shear rigidity of the shear connector is infinite, i.e., $k_s \to \infty$, the continuous condition (15) reduces to the same form as Eq. (16), which corresponds to the full interaction interfaces.

Taking $\zeta = \zeta_i$ in Eq. (11), we have the relation of the state variables at the top and bottom interfaces of element $i$, which is

$$\begin{Bmatrix} U_i(\zeta_i) \\ \sigma_i(\zeta_i) \\ V_i(\zeta_i) \\ \tau_i(\zeta_i) \end{Bmatrix} = [\mathbf{T}_i] \begin{Bmatrix} U_i(\zeta_{i-1}) \\ \sigma_i(\zeta_{i-1}) \\ V_i(\zeta_{i-1}) \\ \tau_i(\zeta_{i-1}) \end{Bmatrix} \quad (i = 1,2,\ldots,m), \tag{17}$$

where the transfer matrix $[\mathbf{T}_i]$ is given by

$$[\mathbf{T}_i] = \exp([\mathbf{K}_i]\Delta\zeta_i) \tag{18}$$

in which $\Delta\zeta_i = h_i/h$ $(i = 1,2,\ldots,m)$. By employing Eqs. (15)–(17), the following relations of the state variables at the top and bottom surfaces of the beam are obtained

$$\begin{Bmatrix} U_m(1) \\ \sigma_m(1) \\ V_m(1) \\ \tau_m(1) \end{Bmatrix} = [\mathbf{T}_m][\mathbf{T}_{m-1}]\cdots[\mathbf{T}_2][\mathbf{P}][\mathbf{T}_1] \begin{Bmatrix} U_1(0) \\ \sigma_1(0) \\ V_1(0) \\ \tau_1(0) \end{Bmatrix}, \tag{19}$$

where the matrix $[\mathbf{P}]$ is the coefficient matrix of Eq. (15).

Because Eq. (19) has four equations with eight variables, complementary conditions are necessary, i.e., the boundary conditions at the top and bottom surfaces of the beam. In the case of buckling or free vibration, these surfaces are traction free, namely,

$$\sigma_y\big|_{y=0} = 0, \quad \sigma_y\big|_{y=h} = 0, \quad \tau_{xy}\big|_{y=0} = 0, \quad \tau_{xy}\big|_{y=h} = 0. \tag{20}$$

This means that

$$\sigma_1(0) = 0, \quad \sigma_m(1) = 0, \quad \tau_1(0) = 0, \quad \tau_m(1) = 0. \tag{21}$$

The substitution of Eq. (21) into Eq. (19) yields

$$\begin{Bmatrix} U_m(1) \\ 0 \\ V_m(1) \\ 0 \end{Bmatrix} = [\mathbf{T}] \begin{Bmatrix} U_1(0) \\ 0 \\ V_1(0) \\ 0 \end{Bmatrix}, \tag{22}$$

where the matrix $[\mathbf{T}] = [\mathbf{T}_m][\mathbf{T}_{m-1}]\cdots[\mathbf{T}_2][\mathbf{P}][\mathbf{T}_1]$. Rearranging the second and fourth ones of the above equation gives

$$\begin{bmatrix} T_{21} & T_{23} \\ T_{41} & T_{43} \end{bmatrix} \begin{Bmatrix} U_1(0) \\ V_1(0) \end{Bmatrix} = \begin{Bmatrix} 0 \\ 0 \end{Bmatrix} \tag{23}$$

in which $T_{ij}$ denotes the element located at the $i$th row and $j$th column of the matrix $[\mathbf{T}]$. For non-trivial solutions of the unknowns $U_1(0)$ and $V_1(0)$, the determinant of the coefficient matrix of Eq. (23) has to vanish, namely,

$$\begin{vmatrix} T_{21} & T_{23} \\ T_{41} & T_{43} \end{vmatrix} = 0. \tag{24}$$

This is the characteristic equation of the buckling or free vibration with initial stress of partial interaction composite beams.

The above derivation shows that the interlayer slip can be considered naturally using the state-space method. Because the hypothesis of the lateral deflection and longitudinal displacement along the thickness of the beam, which is usually introduced in one-dimensional beam theory, is not adopted, the proposed method can be used to find more realistic distributions of the deformation of partial interaction composite beams. As a result, this work is of great interest and importance, because it can verify and validate the reasonability or precision of one-dimensional beam theories.

## 4. SS-DQM solution for beams with general end conditions

If a beam is not simply supported at either end, expansion using the trigonometric function in the $x$ direction as given by Eq. (6) is not applicable. In general, we can separate the time variable $t$ from the space

variables $\xi$ and $\zeta$ as

$$u_i = hU_i(\zeta,\xi)\exp(\mathrm{j}\omega t), \quad \sigma_{yi} = E_0\sigma_i(\zeta,\xi)\exp(\mathrm{j}\omega t),$$
$$v_i = hV_i(\zeta,\xi)\exp(\mathrm{j}\omega t), \quad \tau_{xyi} = E_0\tau_i(\zeta,\xi)\exp(\mathrm{j}\omega t). \tag{25}$$

Substituting this into Eq. (3) gives

$$\frac{\partial}{\partial\zeta}\begin{Bmatrix} U_i \\ \sigma_i \\ V_i \\ \tau_i \end{Bmatrix} = \begin{bmatrix} \mathbf{0} & \mathbf{A}_i \\ \mathbf{B}_i & \mathbf{0} \end{bmatrix}\begin{Bmatrix} U_i \\ \sigma_i \\ V_i \\ \tau_i \end{Bmatrix}, \tag{26}$$

where

$$\mathbf{A}_i = \begin{bmatrix} -s\partial/\partial\xi & 1/\overline{G}_i \\ -\overline{\rho}_i\Omega^2 + \overline{\sigma}^0_{xi}s^2\partial^2/\partial\xi^2 & -s\partial/\partial\xi \end{bmatrix},$$
$$\mathbf{B}_i = \begin{bmatrix} -\mu_i s\partial/\partial\xi & (1-\mu_i^2)/\overline{E}_i \\ -\overline{\rho}_i\Omega^2 + (\overline{\sigma}^0_{xi} - \overline{E}_i)s^2\partial^2/\partial\xi^2 & -\mu_i s\partial/\partial\xi \end{bmatrix}. \tag{27}$$

Eq. (26) will be solved by the semi-analytical method first presented by Chen and co-works [23,24], in which the DQM [26] is used to discretize the $\xi$ direction while the state-space formula is reserved for the $\zeta$ direction. Thus, this method is called the SS-DQM.

The DQM approximates the derivative of a function $f$ at any location $\xi_r$ by a linear summation of all of the functional values $f(\xi_k)$ along a mesh line [26], namely,

$$\frac{\partial^n f(\xi_r)}{\partial\xi^n} = \sum_{k=1}^{N} C^{(n)}_{rk} f(\xi_k) \quad (r = 1,2,\ldots,N), \tag{28}$$

where $N$ is the mesh number and $C^{(n)}_{ik}$ are the weighting coefficients of the $n$th order derivative and can be obtained using the method described in Ref. [26]. The above equation can be rendered in terms of a matrix for convenient coding using a computer language such as MATLAB:

$$\{\mathbf{f}^{(n)}\} = [\mathbf{C}^{(n)}]\{\mathbf{f}\} \tag{29}$$

in which the elements of the matrix $[\mathbf{C}^{(n)}]$ are the coefficients $C^{(n)}_{rk}$ in Eq. (28) and

$$\{\mathbf{f}\} = [f(\xi_1), f(\xi_2), \ldots, f(\xi_N)]^{\mathrm{T}}, \quad \{\mathbf{f}^{(n)}\} = \left[\frac{\partial^n f(\xi_1)}{\partial\xi^n}, \frac{\partial^n f(\xi_2)}{\partial\xi^n}, \ldots, \frac{\partial^n f(\xi_N)}{\partial\xi^n}\right]^{\mathrm{T}}. \tag{30}$$

The $x$ direction of the beam is meshed using $N$ grid points, and the values of the state variables at these grid points are denoted by the vectors $\{\mathbf{U}_i\}$, $\{\mathbf{V}_i\}$, $\{\boldsymbol{\sigma}_i\}$, and $\{\boldsymbol{\tau}_i\}$, namely,

$$\{\mathbf{U}_i\} = [U_i(\zeta,\xi_1), U_i(\zeta,\xi_2), \ldots, U_i(\zeta,\xi_N)]^{\mathrm{T}},$$
$$\{\mathbf{V}_i\} = [V_i(\zeta,\xi_1), V_i(\zeta,\xi_2), \ldots, V_i(\zeta,\xi_N)]^{\mathrm{T}},$$
$$\{\boldsymbol{\sigma}_i\} = [\sigma_i(\zeta,\xi_1), \sigma_i(\zeta,\xi_2), \ldots, \sigma_i(\zeta,\xi_N)]^{\mathrm{T}},$$
$$\{\boldsymbol{\tau}_i\} = [\tau_i(\zeta,\xi_1), \tau_i(\zeta,\xi_2), \ldots, \tau_i(\zeta,\xi_N)]^{\mathrm{T}}. \tag{31}$$

Consequently, the approximation of Eq. (26) in discrete form is

$$\frac{\mathrm{d}}{\mathrm{d}\zeta}\{\mathbf{U}_i\} = -s[\mathbf{C}^{(1)}]\{\mathbf{V}_i\} + \frac{1}{\overline{G}_i}\{\boldsymbol{\tau}_i\},$$
$$\frac{\mathrm{d}}{\mathrm{d}\zeta}\{\boldsymbol{\sigma}_i\} = -\overline{\rho}_i\Omega^2\{\mathbf{V}_i\} + \overline{\sigma}^0_{xi}s^2[\mathbf{C}^{(2)}]\{\mathbf{V}_i\} - s[\mathbf{C}^{(1)}]\{\boldsymbol{\tau}_i\},$$

$$\frac{\mathrm{d}}{\mathrm{d}\zeta}\{\mathbf{V}_i\} = -\mu_i s[\mathbf{C}^{(1)}]\{\mathbf{U}_i\} + \frac{1-\mu_i^2}{\overline{E}_i}\{\boldsymbol{\sigma}_i\},$$
$$\frac{\mathrm{d}}{\mathrm{d}\zeta}\{\boldsymbol{\tau}_i\} = -\overline{\rho}_i\Omega^2\{\mathbf{U}_i\} + (\overline{\sigma}^0_{xi} - \overline{E}_i)s^2[\mathbf{C}^{(2)}]\{\mathbf{U}_i\} - \mu_i s[\mathbf{C}^{(1)}]\{\boldsymbol{\sigma}_i\}. \tag{32}$$

It can also be rewritten in matrix form as

$$\frac{\mathrm{d}}{\mathrm{d}\zeta}\begin{Bmatrix}\mathbf{U}_i\\ \boldsymbol{\sigma}_i\\ \mathbf{V}_i\\ \boldsymbol{\tau}_i\end{Bmatrix} = \begin{bmatrix}\mathbf{0} & \mathbf{0} & -s\mathbf{C}^{(1)} & 1/\overline{G}_i\mathbf{I}\\ \mathbf{0} & \mathbf{0} & -\overline{\rho}_i\Omega^2\mathbf{I} + \overline{\sigma}^0_{xi}s^2\overline{\mathbf{C}}^{(2)} & -s\mathbf{C}^{(1)}\\ -\mu_i s\overline{\mathbf{C}}^{(1)} & (1-\mu_i^2)/\overline{E}_i\mathbf{I} & 0 & 0\\ -\overline{\rho}_i\Omega^2\mathbf{I} + (\overline{\sigma}^0_{xi} - \overline{E}_i)s^2\mathbf{C}^{(2)} & -\mu_i s\mathbf{C}^{(1)} & 0 & 0\end{bmatrix}\begin{Bmatrix}\mathbf{U}_i\\ \boldsymbol{\sigma}_i\\ \mathbf{V}_i\\ \boldsymbol{\tau}_i\end{Bmatrix} \tag{33}$$

in which $[\mathbf{I}]$ is the identity matrix of order $N$. The boundary conditions at $x = 0$ and $l$ must be introduced before solving the above equation. If the boundary conditions at the two ends of the beam are represented by the derived variable $\sigma_x$, they must be replaced by the state variables using Eq. (4). The general end conditions of beams are simply supported (S), clamped (C), or free (F) and there are four combinations in practical engineering: SS, SC, CC, and CF. In the case of an SS beam, for example, the boundary conditions are

$$v_i = 0, \quad \sigma_{xi} = 0 \ \text{ at } \ x = 0 \ \text{ and } \ l. \tag{34}$$

The first condition can be used directly, which implies

$$V_{i1} = V_{iN} = 0, \tag{35}$$

while the second condition must be rewritten according to Eq. (4), namely,

$$\sigma_{xi1} = \overline{E}_i s\left[\mathbf{C}^{(1)}_{1,:}\right]\{\mathbf{U}_i\} + \mu_i\sigma_{i1} = 0, \quad \sigma_{xiN} = \overline{E}_i s\left[\mathbf{C}^{(1)}_{N,:}\right]\{\mathbf{U}_i\} + \mu_i\sigma_{iN} = 0 \tag{36}$$

in which $[\mathbf{C}^{(1)}_{1,:}]$ and $[\mathbf{C}^{(1)}_{N,:}]$ are the first and last (i.e., $N$th ) row of the matrix $[\mathbf{C}^{(1)}]$.

The substitution of the above boundary conditions into Eq. (33) gives

$$\frac{\mathrm{d}}{\mathrm{d}\zeta}\begin{Bmatrix}\mathbf{U}_i\\ \overline{\boldsymbol{\sigma}}_i\\ \overline{\mathbf{V}}_i\\ \boldsymbol{\tau}_i\end{Bmatrix} = \begin{bmatrix}\mathbf{0} & \overline{\mathbf{A}}_i\\ \overline{\mathbf{B}}_i & \mathbf{0}\end{bmatrix}\begin{Bmatrix}\mathbf{U}_i\\ \overline{\boldsymbol{\sigma}}_i\\ \overline{\mathbf{V}}_i\\ \boldsymbol{\tau}_i\end{Bmatrix} = [\overline{\mathbf{K}}_i]\begin{Bmatrix}\mathbf{U}_i\\ \overline{\boldsymbol{\sigma}}_i\\ \overline{\mathbf{V}}_i\\ \boldsymbol{\tau}_i\end{Bmatrix} \tag{37}$$

in which

$$\{\overline{\mathbf{V}}_i\} = [V_i(\zeta,\xi_2), V_i(\zeta,\xi_3), \ldots, V_i(\zeta,\xi_{N-1})]^{\mathrm{T}},$$
$$\{\overline{\boldsymbol{\sigma}}_i\} = [\sigma_i(\zeta,\xi_2), \sigma_i(\zeta,\xi_3), \ldots, \sigma_i(\zeta,\xi_{N-1})]^{\mathrm{T}} \tag{38}$$

and

$$\overline{\mathbf{A}}_i = \begin{bmatrix}-s\mathbf{C}^{(1)}_{:,2:N-1} & 1/\overline{G}_i\mathbf{I}\\ -\overline{\rho}_i\Omega^2\mathbf{I}_{2:N-1,2:N-1} + \overline{\sigma}^0_{xi}s^2\mathbf{C}^{(2)}_{2:N-1,2:N-1} & -s\mathbf{C}^{(1)}_{2:N-1,:}\end{bmatrix},$$
$$\overline{\mathbf{B}}_i = \begin{bmatrix}-\mu_i s\mathbf{C}^{(1)}_{2:N-1,:} & (1-\mu_i^2)/\overline{E}_i\mathbf{I}_{2:N-1,2:N-1}\\ -\overline{\rho}_i\Omega^2 I + \overline{\sigma}^0_{xi}s^2\mathbf{C}^{(2)} + \overline{E}_i s^2(\mathbf{C}^{(1)}_{:,1}\mathbf{C}^{(1)}_{1,:} + \mathbf{C}^{(1)}_{:,N}\mathbf{C}^{(1)}_{N,:} - \mathbf{C}^{(2)}) & -\mu_i s\mathbf{C}^{(1)}_{:,2:N-1}\end{bmatrix} \tag{39}$$

in which some notations of the sub-matrix are introduced for the sake of concise expression. The symbol $\mathbf{C}^{(1)}_{2:N-1,:}$, for example, denotes the sub-matrix of the matrix $[\mathbf{C}^{(1)}]$ from the second row to the $(N-1)$th row. In a

similar manner, the symbol $\mathbf{C}^{(2)}_{2:N-1,2:N-1}$ denotes the sub-matrix from the second row to the $(N-1)$th row and from the second column to the $(N-1)$th column.

In a manner similar to that described in Section 3, we can obtain the following relation from the solution of Eq. (37):

$$\{\overline{\mathbf{R}}_i(\zeta_i)\} = [\overline{\mathbf{T}}_i]\{\overline{\mathbf{R}}_i(\zeta_{i-1})\}, \tag{40}$$

where

$$\begin{aligned} \{\overline{\mathbf{R}}_i\} &= \begin{bmatrix} \mathbf{U}_i^{\mathrm{T}} & \overline{\boldsymbol{\sigma}}_i^{\mathrm{T}} & \overline{\mathbf{V}}_i^{\mathrm{T}} & \boldsymbol{\tau}_i^{\mathrm{T}} \end{bmatrix}^{\mathrm{T}}, \\ [\overline{\mathbf{T}}_i] &= \exp([\overline{\mathbf{K}}_i]\Delta\zeta_i). \end{aligned} \tag{41}$$

The compatible condition at the partial interface is

$$\begin{Bmatrix} \mathbf{U}_2(\zeta_1) \\ \overline{\boldsymbol{\sigma}}_2(\zeta_1) \\ \overline{\mathbf{V}}_2(\zeta_1) \\ \boldsymbol{\tau}_2(\zeta_1) \end{Bmatrix} = \begin{bmatrix} \mathbf{I} & \mathbf{0} & \mathbf{0} & E_0/(k_s h)\mathbf{I} \\ \mathbf{0} & \mathbf{I} & \mathbf{0} & \mathbf{0} \\ \mathbf{0} & \mathbf{0} & \mathbf{I} & \mathbf{0} \\ \mathbf{0} & \mathbf{0} & \mathbf{0} & \mathbf{I} \end{bmatrix} \begin{Bmatrix} \mathbf{U}_1(\zeta_1) \\ \overline{\boldsymbol{\sigma}}_1(\zeta_1) \\ \overline{\mathbf{V}}_1(\zeta_1) \\ \boldsymbol{\tau}_1(\zeta_1) \end{Bmatrix} \text{ or } \{\overline{\mathbf{R}}_2(\zeta_1)\} = [\overline{\mathbf{P}}]\{\overline{\mathbf{R}}_1(\zeta_1)\} \tag{42}$$

and the continuous condition at the full interfaces is

$$\begin{Bmatrix} \mathbf{U}_{i+1}(\zeta_i) \\ \boldsymbol{\sigma}_{i+1}(\zeta_i) \\ \mathbf{V}_{i+1}(\zeta_i) \\ \boldsymbol{\tau}_{i+2}(\zeta_i) \end{Bmatrix} = \begin{Bmatrix} \mathbf{U}_i(\zeta_i) \\ \boldsymbol{\sigma}_i(\zeta_i) \\ \mathbf{V}_i(\zeta_i) \\ \boldsymbol{\tau}_i(\zeta_i) \end{Bmatrix} \text{ or } \{\overline{\mathbf{R}}_{i+1}(\zeta_i)\} = \{\overline{\mathbf{R}}_i(\zeta_i)\} \quad (i = 2, 3, \ldots, m-1). \tag{43}$$

As a result, the following transfer relation is obtained from Eqs. (40), (42), and (43):

$$\{\overline{\mathbf{R}}_m(1)\} = [\overline{\mathbf{T}}_m][\overline{\mathbf{T}}_{m-1}]\cdots[\overline{\mathbf{T}}_2][\overline{\mathbf{P}}][\overline{\mathbf{T}}_1]\{\overline{\mathbf{R}}_1(0)\} = [\overline{\mathbf{T}}]\{\overline{\mathbf{R}}_1(0)\}. \tag{44}$$

The traction-free conditions of the upper and bottom surfaces of the beam mean

$$\{\overline{\boldsymbol{\sigma}}_m(1)\} = \{\overline{\boldsymbol{\sigma}}_1(0)\} = 0, \quad \{\boldsymbol{\tau}_m(1)\} = \{\boldsymbol{\tau}_1(0)\} = 0. \tag{45}$$

The substitution of Eq. (45) into Eq. (44) gives

$$\begin{Bmatrix} \mathbf{U}_m(1) \\ \mathbf{0} \\ \overline{\mathbf{V}}_m(1) \\ \mathbf{0} \end{Bmatrix} = \begin{bmatrix} \overline{\mathbf{T}}_{UU} & \overline{\mathbf{T}}_{U\sigma} & \overline{\mathbf{T}}_{UV} & \overline{\mathbf{T}}_{U\tau} \\ \overline{\mathbf{T}}_{\sigma U} & \overline{\mathbf{T}}_{\sigma\sigma} & \overline{\mathbf{T}}_{\sigma V} & \overline{\mathbf{T}}_{\sigma\tau} \\ \overline{\mathbf{T}}_{VU} & \overline{\mathbf{T}}_{V\sigma} & \overline{\mathbf{T}}_{VV} & \overline{\mathbf{T}}_{V\tau} \\ \overline{\mathbf{T}}_{\tau U} & \overline{\mathbf{T}}_{\tau\sigma} & \overline{\mathbf{T}}_{\tau V} & \overline{\mathbf{T}}_{\tau\tau} \end{bmatrix} \begin{Bmatrix} \mathbf{U}_1(0) \\ \mathbf{0} \\ \overline{\mathbf{V}}_1(0) \\ \mathbf{0} \end{Bmatrix}. \tag{46}$$

Hence, a homogeneous equation can be extracted from the second and fourth equations of Eq. (46):

$$\begin{bmatrix} \overline{\mathbf{T}}_{\sigma U} & \overline{\mathbf{T}}_{\sigma V} \\ \overline{\mathbf{T}}_{\tau U} & \overline{\mathbf{T}}_{\tau V} \end{bmatrix} \begin{Bmatrix} \mathbf{U}_1(0) \\ \overline{\mathbf{V}}_1(0) \end{Bmatrix} = \begin{Bmatrix} \mathbf{0} \\ \mathbf{0} \end{Bmatrix}. \tag{47}$$

The characteristic equation of the free vibration or buckling of partial composite beams is obtained

$$\begin{vmatrix} \overline{\mathbf{T}}_{\sigma U} & \overline{\mathbf{T}}_{\sigma V} \\ \overline{\mathbf{T}}_{\tau U} & \overline{\mathbf{T}}_{\tau V} \end{vmatrix} = 0. \tag{48}$$

For other end conditions, the expression of the matrix $[\overline{\mathbf{K}}_i]$, or its sub-matrices $[\overline{\mathbf{A}}_i]$ or $[\overline{\mathbf{B}}_i]$, and the corresponding compatible condition at the partial interface is different, and is detailed in the Appendix.

## 5. Numerical examples

A concrete–wood composite beam (shown in Fig. 4) is used to demonstrate the presented method. The dimensions and material properties of the beam are given in Fig. 3. The beam is a very slender beam with a depth to span ratio of 1/20. This beam has been used by many other researchers to demonstrate the effectiveness of their methods and for comparison purposes [3,19,23]. For other, less slender beams, the advantage or precision of the presented method will be even greater.

First, the convergent property of the presented semi-analytical method is examined for an SS beam as its exact analytical solution has been obtained in Section 3. Table 1 lists the first 10 frequencies of the SS beam (length of the beam $L = 4$ m) without axial force, which are obtained from the exact analytical method and the semi-analytical method. It shows that the first frequency by the SS-DQM converges to an exact solution when $N = 13$, while the first 10 frequencies converge when $N = 27$.

Tables 2–5 list the first 10 frequencies of the flexural mode for four general end conditions, i.e., SS, SC, CC, and CF. The results based on TBT and CBT [19] are also tabulated for comparison. It can be readily found that the relative errors of the results from CBT increase rapidly with the order of the vibration mode. For the SS and SC beams, the first five frequencies obtained by CBT are precise enough because their relative errors are less than 5%, as are the first five frequencies of the CC beam and the first six frequencies of the CF beam. However, TBT can predict the frequencies more precisely than can CBT. For example, the first nine frequencies of the SS beam using TBT have a small ($<5\%$) relative error, as have the first eight frequencies of the SC and CF beams. It is also found that the end conditions of the composite beams can significantly affect the precision of the frequencies that are based on CBT. The relative error of the 10th frequency of the SC beam is 37.15% whereas that of the SS beam is only 13.22%.

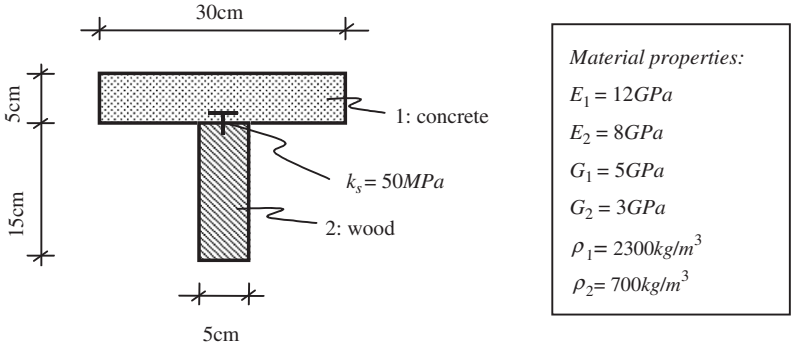


Fig. 4. Dimensions and material properties of a composite beam.

Table 1
The first 10 frequencies of the SS beam using the exact method and SS-DQM (Hz)

| Order | Exact | SS-DQM | | | | | | | |
|---|---|---|---|---|---|---|---|---|---|
| | | $N = 13$ | $N = 15$ | $N = 17$ | $N = 19$ | $N = 21$ | $N = 23$ | $N = 25$ | $N = 27$ |
| 1 | 10.2768 | 10.2768 | 10.2768 | 10.2768 | 10.2768 | 10.2768 | 10.2768 | 10.2768 | 10.2768 |
| 2 | 33.1771 | 33.1771 | 33.1771 | 33.1771 | 33.1771 | 33.1771 | 33.1771 | 33.1771 | 33.1771 |
| 3 | 65.3343 | 65.3343 | 65.3343 | 65.3343 | 65.3343 | 65.3343 | 65.3343 | 65.3343 | 65.3343 |
| 4 | 107.3095 | 107.3078 | 107.3095 | 107.3095 | 107.3095 | 107.3095 | 107.3095 | 107.3095 | 107.3095 |
| 5 | 159.2021 | 159.1080 | 159.2039 | 159.2021 | 159.2021 | 159.2021 | 159.2021 | 159.2021 | 159.2021 |
| 6 | 220.6233 | 222.3699 | 220.6606 | 220.6250 | 220.6233 | 220.6233 | 220.6233 | 220.6233 | 220.6233 |
| 7 | 290.9092 | 279.0055 | 289.4288 | 290.8754 | 290.9056 | 290.9092 | 290.9092 | 290.9092 | 290.9092 |
| 8 | 369.2557 | 444.9911 | 380.3854 | 370.0474 | 369.3018 | 369.2557 | 369.2557 | 369.2557 | 369.2557 |
| 9 | 454.7913 | 464.9695 | 429.3065 | 446.2283 | 454.1611 | 454.7540 | 454.7913 | 454.7913 | 454.7913 |
| 10 | 546.6124 | – | 589.8497 | 586.2463 | 551.9660 | 547.0863 | 546.6248 | 546.6142 | 546.6124 |

Table 2
The first 10 flexural frequencies of the SS beam without axial force (Hz)

| Order | Presented (exact) | Timoshenko's beam theory | | Classical beam theory | |
|---|---|---|---|---|---|
| | | Ref. [19] | Relative error[a] (%) | Ref. [19] | Relative error (%) |
| 1 | 10.2768 | 10.3023 | 0.25 | 10.3215 | 0.43 |
| 2 | 33.1771 | 33.3569 | 0.54 | 33.5264 | 1.05 |
| 3 | 65.3343 | 65.8811 | 0.84 | 66.4831 | 1.76 |
| 4 | 107.3095 | 108.6140 | 1.22 | 110.1706 | 2.67 |
| 5 | 159.2021 | 161.9071 | 1.70 | 165.2736 | 3.81 |
| 6 | 220.6233 | 225.6710 | 2.29 | 232.1107 | 5.21 |
| 7 | 290.9092 | 299.5853 | 2.98 | 310.8313 | 6.85 |
| 8 | 369.2557 | 383.2073 | 3.78 | 401.5099 | 8.73 |
| 9 | 454.7913 | 476.0263 | 4.67 | 504.1863 | 10.86 |
| 10 | 546.6124 | 577.4941 | 5.65 | 618.8832 | 13.22 |

[a]The relative errors are calculated with respect to those of the presented method (column 2).

Table 3
The first 10 flexural frequencies of the SC beam without axial force (Hz)

| Order | Presented ($N = 21$) | Timoshenko's beam theory | | Classical beam theory | |
|---|---|---|---|---|---|
| | | Ref. [19] | Relative error[a] (%) | Ref. [19] | Relative error (%) |
| 1 | 14.1376 | 14.1997 | 0.44 | 14.2548 | 0.83 |
| 2 | 38.9602 | 39.2428 | 0.73 | 39.5421 | 1.49 |
| 3 | 73.4855 | 74.2380 | 1.02 | 75.1940 | 2.32 |
| 4 | 117.8677 | 119.2515 | 1.17 | 121.8482 | 3.38 |
| 5 | 171.9755 | 180.1912 | 4.78 | 180.0027 | 4.67 |
| 6 | 235.3138 | 243.7934 | 3.60 | 249.9127 | 6.20 |
| 7 | 307.2026 | 320.0819 | 4.19 | 331.7072 | 7.98 |
| 8 | 386.9124 | 406.1931 | 4.98 | 425.4547 | 9.96 |
| 9 | 447.2454 | 501.4575 | 12.12 | 531.1936 | 18.77 |
| 10 | 473.1775 | – | – | 648.9469 | 37.15 |

[a]The relative errors are calculated with respect to those of the presented method (column 2).

Table 4
The first 10 flexural frequencies of the CC beam without axial force (Hz)

| Order | Presented ($N = 21$) | Timoshenko's beam theory | | Classical beam theory | |
|---|---|---|---|---|---|
| | | Ref. [19] | Relative error[a] (%) | Ref. [19] | Relative error (%) |
| 1 | 18.5859 | 18.6965 | 0.59 | 18.8059 | 1.18 |
| 2 | 45.2227 | 45.6429 | 0.93 | 46.1245 | 1.99 |
| 3 | 82.2490 | 83.2140 | 1.17 | 84.6717 | 2.95 |
| 4 | 128.9548 | 129.9440 | 0.77 | 134.3068 | 4.15 |
| 5 | 185.1945 | 195.5333 | 5.58 | 195.5276 | 5.58 |
| 6 | 250.3416 | 262.3964 | 4.82 | 268.5035 | 7.25 |
| 7 | 323.9593 | 341.2276 | 5.33 | 353.3696 | 9.08 |
| 8 | 404.6205 | 429.8477 | 6.23 | 450.1800 | 11.26 |
| 9 | 489.2047 | – | – | 558.9783 | 14.26 |
| 10 | 584.7517 | – | – | 679.7840 | 16.25 |

[a]The relative errors are calculated with respect to those of the presented method (column 2).

The presented method is also applicable for the buckling analysis of partial interaction composite beams, simply by letting the density of the material equal to zero. Tables 6–8 provide the first five buckling loads for the SS, SC, and CC beams. The numerical results show that those of TBT are precise enough for a slender

Table 5
The first 10 flexural frequencies of the CF beam without axial force (Hz)

| Order | Presented ($N = 21$) | Timoshenko's beam theory | | Classical beam theory | |
|---|---|---|---|---|---|
| | | Ref. [19] | Relative error[a] (%) | Ref. [19] | Relative error (%) |
| 1 | 3.9913 | 3.9935 | 0.06 | 3.9976 | 0.16 |
| 2 | 20.0468 | 20.0936 | 0.23 | 20.1865 | 0.70 |
| 3 | 48.4782 | 48.7483 | 0.56 | 49.1650 | 1.42 |
| 4 | 85.9909 | 86.3573 | 0.43 | 87.6023 | 1.87 |
| 5 | 132.2778 | 133.6544 | 1.04 | 137.1518 | 3.68 |
| 6 | 189.6269 | 195.7206 | 3.21 | 198.1001 | 4.47 |
| 7 | 252.9368 | 263.5636 | 4.20 | 270.8708 | 7.09 |
| 8 | 328.5248 | 342.2862 | 4.19 | 355.5156 | 8.22 |
| 9 | 405.6944 | 430.7051 | 6.16 | 452.1544 | 11.45 |
| 10 | 447.7495 | – | – | 560.7886 | 25.25 |

[a]The relative errors are calculated with respect to those of the presented method (column 2).

Table 6
The first five buckling loads of the SS beam (kN)

| Order | Presented (exact) | Timoshenko's beam theory | | Classical beam theory | |
|---|---|---|---|---|---|
| | | Ref. [19] | Relative error[a] (%) | Ref. [19] | Relative error (%) |
| 1 | 268.6351 | 270.0838 | 0.54 | 271.0222 | 0.89 |
| 2 | 699.6742 | 708.3848 | 1.24 | 714.8772 | 2.17 |
| 3 | 1205.0415 | 1229.6902 | 2.05 | 1249.3871 | 3.68 |
| 4 | 1826.8929 | 1883.2759 | 3.09 | 1929.8718 | 5.64 |
| 5 | 2570.9989 | 2683.9653 | 4.39 | 2779.6112 | 8.11 |

[a]The relative errors are calculated with respect to those of the presented method (column 2).

Table 7
The first five buckling loads of the SC beam (kN)

| Order | Presented ($N = 21$) | Timoshenko's beam theory | | Classical beam theory | |
|---|---|---|---|---|---|
| | | Ref. [19] | Relative error[a] (%) | Ref. [19] | Relative error (%) |
| 1 | 437.7220 | 441.7282 | 0.92 | 444.2441 | 1.49 |
| 2 | 911.2396 | 926.1098 | 1.63 | 937.2378 | 2.85 |
| 3 | 1477.3659 | 1514.8872 | 2.54 | 1544.8915 | 4.57 |
| 4 | 2163.7066 | 2244.0444 | 3.71 | 2310.5175 | 6.79 |
| 5 | 2966.8595 | 3119.7055 | 5.15 | 3249.6805 | 9.53 |

[a]The relative errors are calculated with respect to those of the presented method (column 2).

Table 8
The first five buckling loads of the CC beam (kN)

| Order | Presented ($N = 21$) | Timoshenko's beam theory | | Classical beam theory | |
|---|---|---|---|---|---|
| | | Ref. [19] | Relative error[a] (%) | Ref. [19] | Relative error (%) |
| 1 | 699.8523 | 708.3848 | 1.22 | 714.8772 | 2.15 |
| 2 | 1109.0655 | 1132.2174 | 2.09 | 1148.8943 | 3.59 |
| 3 | 1827.4148 | 1883.2759 | 3.06 | 1929.8718 | 5.61 |
| 4 | 2494.8894 | 2605.5477 | 4.44 | 2695.5925 | 8.04 |
| 5 | 3426.6865 | 3630.0124 | 5.93 | 3807.1939 | 11.10 |

[a]The relative errors are calculated with respect to those of the presented method (column 2).

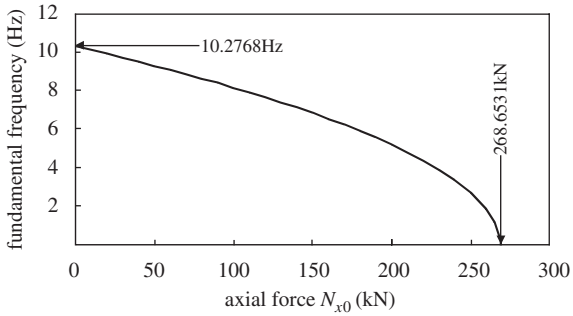


Fig. 5. The fundamental frequency of the SS beam with axial force.

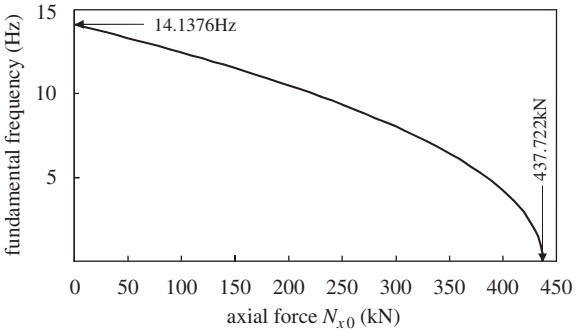


Fig. 6. The fundamental frequency of the SC beam with axial force.

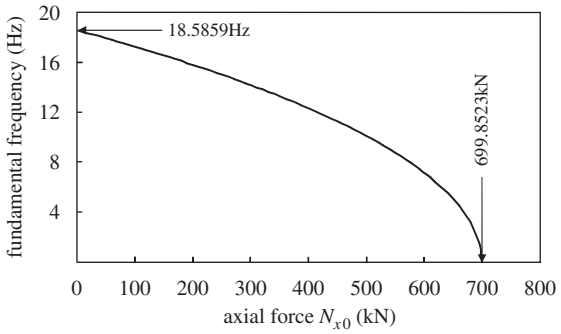


Fig. 7. The fundamental frequency of the CC beam with axial force.

composite beam ($h/L = 1/20$). However, CBT can predict only the first two or three buckling loads with a small relative error ($<5\%$).

Moreover, the presented method can be used to study the free vibration of composite beams with axial force. Fig. 5 plots the fundamental frequency of the SS beam, which decreases with the axial force and which vanishes if the axial force reaches critical loading. Figs. 6 and 7 show the same phenomenon of the variation of the fundamental frequency due to axial force in the SC and CC beams.

## 6. Conclusions

A two-dimensional theory is presented to investigate the free vibration and buckling behavior of partial composite beams. The exact analytical solution for simply supported beams is obtained, as well as

semi-analytical solutions for general end conditions. Unlike beam theories, the presented method does not impose extra restriction or assumption on the deflection and longitudinal displacement along the thickness of the beam. As a result, the presented model is more precise and realistic than models based on beam theory, whether CBT or shear deformable beam theories (e.g. TBT and other high order shear deformation beam theories). Consequently, the results of the presented method can be the benchmark for other approximate analytical and numerical methods based on one-dimensional beam theories.

**Acknowledgement**

The work described in this paper was fully supported by a grant from the Research Grants Council of the Hong Kong Special Administrative Region, China (Project no. CityU 122106).

**Appendix**

For a CF beam, the modified state-space formula considering the boundary conditions is

$$\frac{\mathrm{d}}{\mathrm{d}\zeta}\begin{Bmatrix}\overline{\mathbf{U}}_i\\ \overline{\boldsymbol{\sigma}}_i\\ \overline{\mathbf{V}}_i\\ \overline{\boldsymbol{\tau}}_i\end{Bmatrix}=\begin{bmatrix}\mathbf{0} & \overline{\mathbf{A}}_i\\ \overline{\mathbf{B}}_i & \mathbf{0}\end{bmatrix}\begin{Bmatrix}\overline{\mathbf{U}}_i\\ \overline{\boldsymbol{\sigma}}_i\\ \overline{\mathbf{V}}_i\\ \overline{\boldsymbol{\tau}}_i\end{Bmatrix}=[\overline{\mathbf{K}}_i]\begin{Bmatrix}\overline{\mathbf{U}}_i\\ \overline{\boldsymbol{\sigma}}_i\\ \overline{\mathbf{V}}_i\\ \overline{\boldsymbol{\tau}}_i\end{Bmatrix}, \tag{A.1}$$

where

$$\begin{aligned}\{\overline{\mathbf{U}}_i\}&=[U_i(\zeta,\xi_2),U_i(\zeta,\xi_3),\ldots,U_i(\zeta,\xi_N)]^{\mathrm{T}},\\ \{\overline{\boldsymbol{\sigma}}_i\}&=[\sigma_i(\zeta,\xi_1),\sigma_i(\zeta,\xi_2),\ldots,\sigma_i(\zeta,\xi_{N-1})]^{\mathrm{T}},\\ \{\overline{\mathbf{V}}_i\}&=[V_i(\zeta,\xi_2),V_i(\zeta,\xi_3),\ldots,V_i(\zeta,\xi_N)]^{\mathrm{T}},\\ \{\overline{\boldsymbol{\tau}}_i\}&=[\tau_i(\zeta,\xi_1),\tau_i(\zeta,\xi_2),\ldots,\tau_i(\zeta,\xi_{N-1})]^{\mathrm{T}}\end{aligned} \tag{A.2}$$

and

$$\begin{aligned}\overline{\mathbf{A}}_i&=\begin{bmatrix}-s\mathbf{C}^{(1)}_{2:N,2:N} & 1/\overline{G}_i\mathbf{I}_{2:N,1:N-1}\\ -\overline{\rho}_i\Omega^2\mathbf{I}_{1:N-1,2:N}+\overline{\sigma}^0_{xi}s^2\mathbf{C}^{(2)}_{1:N-1,2:N} & -s\mathbf{C}^{(1)}_{1:N-1,1:N-1}\end{bmatrix},\\ \overline{\mathbf{B}}_i&=\begin{bmatrix}-\mu_i s\mathbf{C}^{(1)}_{2:N,2:N}-s(1-\mu_i^2)/\mu_i\mathbf{I}_{2:N,N}\mathbf{C}^{(1)}_{N,2:N} & (1-\mu_i^2)/\overline{E}_i\mathbf{I}_{2:N,1:N-1}\\ -\overline{\rho}_i\Omega^2\mathbf{I}_{1:N-1,2:N}+(\overline{\sigma}^0_{xi}-\bar{E}_i)s^2\mathbf{C}^{(2)}_{1:N-1,2:N}+\overline{E}_i s^2\mathbf{C}^{(1)}_{1:N-1,N}\mathbf{C}^{(1)}_{N,2:N} & -\mu_i s\mathbf{C}^{(1)}_{1:N-1,2:N-1}\end{bmatrix}.\end{aligned} \tag{A.3}$$

The corresponding compatible conditions at the partial interaction interface are

$$\begin{Bmatrix}\overline{\mathbf{U}}_2(\zeta_1)\\ \overline{\boldsymbol{\sigma}}_2(\zeta_1)\\ \overline{\mathbf{V}}_2(\zeta_1)\\ \overline{\boldsymbol{\tau}}_2(\zeta_1)\end{Bmatrix}=\begin{bmatrix}\mathbf{I} & \mathbf{0} & \mathbf{0} & E_0/(k_s h)\mathbf{I}_{2:N,1:N-1}\\ \mathbf{0} & \mathbf{I} & \mathbf{0} & \mathbf{0}\\ \mathbf{0} & \mathbf{0} & \mathbf{I} & \mathbf{0}\\ \mathbf{0} & \mathbf{0} & \mathbf{0} & \mathbf{I}\end{bmatrix}\begin{Bmatrix}\overline{\mathbf{U}}_1(\zeta_1)\\ \overline{\sigma}_1(\zeta_1)\\ \overline{\mathbf{V}}_1(\zeta_1)\\ \overline{\boldsymbol{\tau}}_1(\zeta_1)\end{Bmatrix}. \tag{A.4}$$

For a CC beam, the modified state-space formula considering the end conditions is

$$\frac{\mathrm{d}}{\mathrm{d}\zeta}\begin{Bmatrix}\overline{\mathbf{U}}_i\\ \boldsymbol{\sigma}_i\\ \overline{\mathbf{V}}_i\\ \boldsymbol{\tau}_i\end{Bmatrix}=\begin{bmatrix}\mathbf{0} & \overline{\mathbf{A}}_i\\ \overline{\mathbf{B}}_i & \mathbf{0}\end{bmatrix}\begin{Bmatrix}\overline{\mathbf{U}}_i\\ \boldsymbol{\sigma}_i\\ \overline{\mathbf{V}}_i\\ \boldsymbol{\tau}_i\end{Bmatrix}=[\overline{\mathbf{K}}_i]\begin{Bmatrix}\overline{\mathbf{U}}_i\\ \boldsymbol{\sigma}_i\\ \overline{\mathbf{V}}_i\\ \boldsymbol{\tau}_i\end{Bmatrix}, \tag{A.5}$$

where

$$\begin{aligned}\{\overline{\mathbf{U}}_i\} &= [U_i(\zeta,\xi_2), U_i(\zeta,\xi_3),\ldots, U_i(\zeta,\xi_{N-1})]^{\mathrm{T}},\\ \{\overline{\mathbf{V}}_i\} &= [V_i(\zeta,\xi_2), V_i(\zeta,\xi_3),\ldots, V_i(\zeta,\xi_{N-1})]^{\mathrm{T}}\end{aligned} \tag{A.6}$$

and

$$\begin{aligned}\overline{\mathbf{A}}_i &= \begin{bmatrix} -s\mathbf{C}^{(1)}_{2:N-1,2:N-1} & 1/\overline{G}_i\mathbf{I}_{2:N-1,:}\\ -\overline{\rho}_i\Omega^2\mathbf{I}_{:,2:N-1}+\overline{\sigma}^0_{xi}s^2\mathbf{C}^{(2)}_{:,2:N-1} & -s\mathbf{C}^{(1)}\end{bmatrix},\\ \overline{\mathbf{B}}_i &= \begin{bmatrix} -\mu_i s\mathbf{C}^{(1)}_{2:N-1,2:N-1} & (1-\mu_i^2)/\overline{E}_i\mathbf{I}_{2:N-1,:}\\ -\overline{\rho}_i\Omega^2\mathbf{I}_{:,2:N-1}+(\overline{\sigma}^0_{xi}-\overline{E}_i)s^2\mathbf{C}^{(2)}_{:,2:N-1} & -\mu_i s\mathbf{C}^{(1)}\end{bmatrix}.\end{aligned} \tag{A.7}$$

The corresponding compatible conditions at the partial interaction interface are

$$\begin{Bmatrix}\overline{\mathbf{U}}_2(\zeta_1)\\ \overline{\boldsymbol{\sigma}}_2(\zeta_1)\\ \overline{\mathbf{V}}_2(\zeta_1)\\ \overline{\boldsymbol{\tau}}_2(\zeta_1)\end{Bmatrix} = \begin{bmatrix}\mathbf{I} & \mathbf{0} & \mathbf{0} & E_0/(k_sh)\mathbf{I}_{2:N-1,:}\\ \mathbf{0} & \mathbf{I} & \mathbf{0} & \mathbf{0}\\ \mathbf{0} & \mathbf{0} & \mathbf{I} & \mathbf{0}\\ \mathbf{0} & \mathbf{0} & \mathbf{0} & \mathbf{I}\end{bmatrix}\begin{Bmatrix}\overline{\mathbf{U}}_1(\zeta_1)\\ \overline{\boldsymbol{\sigma}}_1(\zeta_1)\\ \overline{\mathbf{V}}_1(\zeta_1)\\ \overline{\boldsymbol{\tau}}_1(\zeta_1)\end{Bmatrix}. \tag{A.8}$$

For an SC beam, the modified state-space formula considering the end boundary conditions is

$$\frac{\mathrm{d}}{\mathrm{d}\zeta}\begin{Bmatrix}\overline{\mathbf{U}}_i\\ \overline{\boldsymbol{\sigma}}_i\\ \overline{\mathbf{V}}_i\\ \boldsymbol{\tau}_i\end{Bmatrix} = \begin{bmatrix}\mathbf{0} & \overline{\mathbf{A}}_i\\ \overline{\mathbf{B}}_i & \mathbf{0}\end{bmatrix}\begin{Bmatrix}\overline{\mathbf{U}}_i\\ \overline{\boldsymbol{\sigma}}_i\\ \overline{\mathbf{V}}_i\\ \boldsymbol{\tau}_i\end{Bmatrix} = [\overline{\mathbf{K}}_i]\begin{Bmatrix}\overline{\mathbf{U}}_i\\ \overline{\boldsymbol{\sigma}}_i\\ \overline{\mathbf{V}}_i\\ \boldsymbol{\tau}_i\end{Bmatrix}, \tag{A.9}$$

where

$$\begin{aligned}\{\overline{\mathbf{U}}_i\} &= [U_i(\zeta,\xi_1), U_i(\zeta,\xi_2),\ldots, U_i(\zeta,\xi_{N-1})]^{\mathrm{T}},\\ \{\overline{\boldsymbol{\sigma}}_i\} &= [\sigma_i(\zeta,\xi_2), \sigma_i(\zeta,\xi_3),\ldots, \sigma_i(\zeta,\xi_N)]^{\mathrm{T}},\\ \{\overline{\mathbf{V}}_i\} &= [V_i(\zeta,\xi_2), V_i(\zeta,\xi_3),\ldots, V_i(\zeta,\xi_{N-1})]^{\mathrm{T}}\end{aligned} \tag{A.10}$$

and

$$\begin{aligned}\overline{\mathbf{A}}_i &= \begin{bmatrix} -s\mathbf{C}^{(1)}_{1:N-1,2:N-1} & 1/\overline{G}_i\mathbf{I}_{1:N-1,:}\\ -\overline{\rho}_i\Omega^2\mathbf{I}_{2:N,2:N-1}+\overline{\sigma}^0_{xi}s^2\mathbf{C}^{(2)}_{2:N,2:N-1} & -s\mathbf{C}^{(1)}_{2:N,:}\end{bmatrix},\\ \overline{\mathbf{B}}_i &= \begin{bmatrix} -\mu_i s\mathbf{C}^{(1)}_{2:N-1,1:N-1} & (1-\mu_i^2)/\overline{E}_i\mathbf{I}_{2:N-1,2:N}\\ -\overline{\rho}_i\Omega^2\mathbf{I}_{:,1:N-1}+(\overline{\sigma}^0_{xi}-\overline{E}_i)s^2\mathbf{C}^{(2)}_{:,1:N-1}+\overline{E}_i s^2\mathbf{C}^{(1)}_{:,1}\mathbf{C}^{(1)}_{1,1:N-1} & -\mu_i s\mathbf{C}^{(1)}_{:,2:N}\end{bmatrix}.\end{aligned} \tag{A.11}$$

The corresponding compatible conditions at the partial interaction interface are

$$\begin{Bmatrix}\overline{\mathbf{U}}_2(\zeta_1)\\ \overline{\boldsymbol{\sigma}}_2(\zeta_1)\\ \overline{\mathbf{V}}_2(\zeta_1)\\ \boldsymbol{\tau}_2(\zeta_1)\end{Bmatrix} = \begin{bmatrix}\mathbf{I} & \mathbf{0} & \mathbf{0} & E_0/(k_sh)\mathbf{I}_{2:N-1,:}\\ \mathbf{0} & \mathbf{I} & \mathbf{0} & \mathbf{0}\\ \mathbf{0} & \mathbf{0} & \mathbf{I} & \mathbf{0}\\ \mathbf{0} & \mathbf{0} & \mathbf{0} & \mathbf{I}\end{bmatrix}\begin{Bmatrix}\overline{\mathbf{U}}_1(\zeta_1)\\ \overline{\boldsymbol{\sigma}}_1(\zeta_1)\\ \overline{\mathbf{V}}_1(\zeta_1)\\ \boldsymbol{\tau}_1(\zeta_1)\end{Bmatrix}. \tag{A.12}$$

## References


[1] N.M. Newmark, C.P. Siess, I.M. Viest, Test and analysis of composite beams with incomplete interaction, *Proceedings of the Society for Experimental Stress and Analysis* 9 (1951) 75–92.

[2] J.R. Goodman, Layered Wood Systems with Interlayer Slip, PhD Thesis, University of California, Berkeley, CA, 1967.

[3] U.A. Girhammar, V.K.A. Gopu, Composite beam-columns with interlayer slip-exact analysis, *Journal of Structural Engineering* 119 (1993) 1265–1282.

[4] U.A. Girhammar, D. Pan, Dynamic analysis of composite members with interlayer slip, *International Journal of Solids and Structures* 30 (1993) 797–823.

[5] U.A. Girhammar, D.H. Pan, Exact static analysis of partially composite beams and beam-columns, *International Journal of Mechanical Sciences* 49 (2007) 239–255.

[6] Y.C. Wang, Deflection of steel–concrete composite beams with partial shear interaction, *Journal of Structural Engineering* 124 (1998) 1159–1165.

[7] G. Biscontin, A. Morassi, P. Wendel, Vibrations of steel–concrete composite beams, *Journal of Vibration and Control* 6 (2000) 691–714.

[8] G. Ranzi, M.A. Bradford, Analytical solutions for elevated-temperature behavior of composite beams with partial interaction, *Journal of Structural Engineering* 133 (2007) 788–799.

[9] Y.F. Wu, R.Q. Xu, W.Q. Chen, Free vibration of partial interaction composite members with axial force, *Journal of Sound and Vibration* 299 (2007) 1074–1093.

[10] Y.F. Wu, D.J. Oehlers, M.C. Griffith, Partial-interaction analysis of composite beam/column members, *Mechanics of Structures and Machines* 30 (2002) 309–332.

[11] W.Q. Chen, Y.F. Wu, R.Q. Xu, State space formulation for composite beam-columns with partial interaction, *Composites Science and Technology* 67 (2007) 2500–2512.

[12] E.J. Amana, L.G. Booth, Theoretical and experimental studies of nailed and glued stressed-skin components, *Journal of Wood Science* 4 (1967) 43–69.

[13] Y.F. Wu, M.C. Griffith, D.J. Oehlers, Improving the strength and ductility of rectangular reinforced concrete columns through composite partial interaction: tests, *Journal of Structural Engineering* 129 (2003) 1183–1190.

[14] L.X. Fang, S.L. Chan, Y.L. Wong, Numerical analysis of composite frames with partial shear–stud interaction by one element per member, *Engineering Structures* 22 (2000) 1285–1300.

[15] M.R. Salari, E. Spacone, Finite element formulations of one-dimensional elements with bond-slip, *Engineering Structures* 23 (2001) 815–826.

[16] G. Ranzi, M.A. Bradford, B. Uy, A direct stiffness analysis of a composite beam with partial interaction, *International Journal of Numerical Methods in Engineering* 61 (2004) 657–672.

[17] Y.F. Wu, M.C. Griffith, D.J. Oehlers, Numerical simulation of steel plated RC column, *Computers and Structures* 82 (2004) 359–371.

[18] S. Schnabl, M. Saje, G. Turk, I. Planinc, Analytical solution of two-layer beam taking into account interlayer slip and shear deformation, *Journal of Structural Engineering* 133 (2007) 886–894.

[19] R.Q. Xu, Y.F. Wu, Static, dynamic, and buckling analysis of partial interaction composite members using Timoshenko's beam theory, *International Journal of Mechanical Sciences* (2007).

[20] S. Berczynski, T.T. Wrsblewski, Vibration of steel–concrete composite beams using the Timoshenko beam model, *Journal of Vibration and Control* 11 (2005) 829–848.

[21] G. Ranzi, A. Zona, A composite beam model including the shear deformability of the steel component, *Engineering Structures* 29 (2007) 3026–3041.

[22] R.Q. Xu, Y.F. Wu, Two-dimensional analytical solutions of simply supported composite beams with interlayer slips, *International Journal of Solids and Structures* 44 (2007) 165–175.

[23] W.Q. Chen, C.F. Lv, Z.G. Bian, Elasticity solution for free vibration of laminated beams, *Composite Structures* 62 (2003) 75–82.

[24] W.Q. Chen, K.Y. Lee, On free vibration of cross-ply laminates in cylindrical bending, *Journal of Sound and Vibration* 273 (2004) 667–676.

[25] R.Q. Xu, H.J. Ding, Two-dimensional solutions for orthotropic materials by the state space method, *Composite Structures* 78 (2007) 325–336.

[26] C. Shu, *Differential Quadrature and its Application in Engineering*, Springer, Berlin, 2000.